

## Unraveling Quasiperiodic Relaxations of Transport Barriers with Gyrokinetic Simulations of Tokamak Plasmas

A. Strugarek,<sup>1,2,\*</sup> Y. Sarazin,<sup>1</sup> D. Zarzoso,<sup>1</sup> J. Abiteboul,<sup>1</sup> A. S. Brun,<sup>2</sup> T. Cartier-Michaud,<sup>1</sup> G. Dif-Pradalier,<sup>1</sup> X. Garbet,<sup>1</sup> Ph. Ghendrih,<sup>1</sup> V. Grandgirard,<sup>1</sup> G. Latu,<sup>1</sup> C. Passeron,<sup>1</sup> and O. Thomine<sup>1</sup>

<sup>1</sup>CEA, IRFM, F-13108 Saint-Paul-les-Durance, France

<sup>2</sup>Laboratoire AIM Paris-Saclay, CEA/Irfu Université Paris-Diderot CNRS/INSU, F-91191 Gif-sur-Yvette, France

(Received 25 September 2012; published 2 October 2013)

The generation and dynamics of transport barriers governed by sheared poloidal flows are analyzed in flux-driven 5D gyrokinetic simulations of ion temperature gradient driven turbulence in tokamak plasmas. The transport barrier is triggered by a vorticity source that polarizes the system. The chosen source captures characteristic features of some experimental scenarios, namely, the generation of a sheared electric field coupled to anisotropic heating. For sufficiently large shearing rates, turbulent transport is suppressed and a transport barrier builds up, in agreement with the common understanding of transport barriers. The vorticity source also governs a secondary instability—driven by the temperature anisotropy ( $T_{\parallel} \neq T_{\perp}$ ). Turbulence and its associated zonal flows are generated in the vicinity of the barrier, destroying the latter due to the screening of the polarization source by the zonal flows. These barrier relaxations occur quasiperiodically, and generically result from the decoupling between the dynamics of the barrier generation, triggered by the source driven sheared flow, and that of the crash, triggered by the secondary instability. This result underlines that barriers triggered by sheared flows are prone to relaxations whenever secondary instabilities come into play.

DOI: [10.1103/PhysRevLett.111.145001](https://doi.org/10.1103/PhysRevLett.111.145001)

PACS numbers: 52.65.Tt, 52.30.Gz, 52.35.Ra, 52.35.We

Heat transport in controlled fusion devices like tokamaks is mainly governed by turbulence. Any control, even partial, of the turbulent transport level is highly desirable in view of improving discharge performance and ultimately reducing the total cost of this carbon-free energy source. In this context, large scale sheared flows have been proven efficient in reducing the magnitude of turbulent transport in plasmas, both through vortex stretching and nonlinear decorrelation [1], and possibly in lowering the linear drive of the main instability at the origin of the turbulent transport [2]. These mechanisms are also encountered in neutral fluids [3], especially in planetary atmospheres such as Jupiter [4] or Earth [5]. They also bear analogy with sheared self-organized critical models [6]. In tokamaks, turbulent eddies essentially rotate in the poloidal direction which encircles the magnetic axis at a speed proportional to the radial electric field  $E_r$ , the radius being the direction of confinement [7,8]. Sheared poloidal flows, or equivalently sheared  $E_r$ , can efficiently improve the confinement. They are likely key ingredients to trigger bifurcations towards transport barriers (TBs) [9] which are essential for reference scenario for ITER [10]. Interestingly, the associated TBs may exhibit time-dependent behaviors such as relaxation processes [11]. Stationary large scale poloidal flows contribute to the radial force balance through the Lorentz force. They can be driven by specific external anisotropic heating schemes such as so-called ion Bernstein wave heating (IBWH), which lead to both the generation of radial electric field and to anisotropic ion temperatures due to preferential transverse—to

**B**—heating ( $T_{\parallel} \neq T_{\perp}$ ), with **B** the equilibrium magnetic field [12]. Also, small scale turbulence is well known to excite both large scale zonal (low frequency) [13] and mean (stationary) flows [14], the interplay of which is nontrivial [15–18].

There are numerous experimental and theoretical evidences of turbulence regulation by sheared poloidal flows. Several fluid simulations in the flux-driven regime have also reported such transitions [19,20]. In this Letter, we report for the first time on the observation of TB generation in flux-driven gyrokinetic global simulations of ion temperature gradient (ITG) driven turbulence. It appears that the dynamics of these TBs exhibits quasiperiodic crashes, which are found to result from the complex interplay between the unavoidable kinetic properties of any polarization source and the backreaction of turbulence.

Studying TB formation in numerical simulations requires the control to some extent of the shearing rate level. When conducting such experiments in fluid [20] or local slab gyrokinetic [21] simulations by prescribing the asymptotic shearing magnitude, TBs were created. Fluid simulations [20] reported that the time delay of the stabilizing effect from the shearing rate resulted in the transient growth of resonant modes and subsequently in quasiperiodic relaxations of the TBs. More recent gyrokinetic simulations with arbitrary flow profiles also report turbulence suppression above a certain threshold in shearing rate [22]. Unlike previous gyrokinetic simulations [21,22], our study shows how turbulence and transport self-consistently organize themselves on typical energy confinement times

in the *flux driven* regime, when both heat and vorticity sources keep the system out of thermodynamical equilibrium. In turn, the maximal shear of  $E_r$  increases with the vorticity source magnitude, up to a point where a TB is quasiperiodically triggered. Two critical results are obtained: (i) an ion TB is triggered, provided the shearing rate exceeds some threshold which increases with the heating source, and (ii) this TB exhibits quasiperiodic crashes, which result from the transient screening of the vorticity source by the turbulence-induced zonal and mean flows.

The flux-driven code GYSELA [23] is used to study the interaction of TBs with both local and nonlocal turbulent effects, as well as large-scale mean and zonal flow generation and mean equilibrium evolution. It solves the 5D ion gyrokinetic equation for the full distribution function  $\bar{F}$  of the ion guiding centers (no scale separation is assumed between equilibrium and fluctuations):

$$\partial_t \bar{F} + \frac{1}{B_{\parallel}^*} \nabla_{\mathbf{z}} \cdot (\dot{\mathbf{z}} B_{\parallel}^* \bar{F}) = \mathcal{C}(\bar{F}) + \mathcal{S}_{\omega} + \mathcal{S}_{\varepsilon}, \quad (1)$$

where  $\mathbf{z} = (\chi, \theta, \varphi, v_{G\parallel}, \mu)$  and  $\dot{\mathbf{z}} = d_t \mathbf{z}$  (the magnetic flux surface label  $\chi$  labels the radial position in GYSELA, where the torus cross section is circular).  $B_{\parallel}^* = B(1 + J_{\parallel} v_{G\parallel}/B^2)$  is the Jacobian of the gyrocenter transformation ( $J_{\parallel}$  is the parallel current). The collision operator  $\mathcal{C}$  is a reduced Fokker-Planck operator with an isotropic distribution function kernel [24].  $\mathcal{S}_{\omega}$  is a source of vorticity defined hereafter, and the heat source  $\mathcal{S}_{\varepsilon}$  localized at the inner edge of the system sustains the mean temperature on energy confinement times [8]. The quasineutrality constraint closes the system

$$-\sum_{\text{ion species}} \nabla \cdot \left( \frac{n_{\text{eq},s} m_s}{\mathbf{B}^2} \nabla_{\perp} \phi \right) = \sum_{\text{species}} q_s \int d\nu^* J \cdot \bar{F}. \quad (2)$$

$J$  is the gyro-averaging operator [approximated by  $(1 - (m_s/2q_s^2 B_0) \mu \nabla_{\perp}^2)^{-1}$  in GYSELA],  $n_{\text{eq}}$  the equilibrium density,  $\phi$  the electrostatic potential and  $d\nu^* = 2\pi B_{\parallel}^* d\mu dv_{G\parallel}$  the integration element in velocity space. An adiabatic response of the electrons is assumed, so that the electron channel for heat transport is precluded.

The vorticity  $W$  is defined as the flux surface average of the left-hand side of (2),

$$W \equiv - \left\langle \nabla \cdot \left( \frac{n_{\text{eq},s} m_s}{\mathbf{B}^2} \nabla_{\perp} \phi \right) \right\rangle_{\text{fs}}. \quad (3)$$

It is clear from Eq. (2) that  $W$  also relates to the gyro-average of the guiding-center distribution function:  $W = e \langle \int d\nu^* J \cdot \bar{F} \rangle_{\text{fs}}$ . This property allows one to partially control the electric field within the gyrokinetic framework, despite the absence of an explicit time evolution equation for the electric field (unlike the fluid approach). Indeed, it then suffices to add a source term  $S$  in Eq. (1), for which the only nonvanishing fluid moment is  $J \cdot S$ . This is exactly

what the vorticity source  $S_{\omega}$  does. Notice that simply adding a prescribed external electric potential in the quasineutrality reveals inefficiencies, since the system then rapidly backreacts and screens the externally imposed potential.

From the expressions of  $W$  and of the  $J$  operator, it is clear that polarizing the plasma through vorticity injection either requires the injection of perpendicular energy and/or of gyrocenters. This intrinsic property is therefore not artificial: it holds for all vorticity sources originating from any physical effect. In IBW experiments, vorticity is deposited through wave-plasma interaction along with energy, and without any source of gyrocenter density. In addition, it is worth noting that IBW heating is inherently anisotropic, hence leading to different parallel and transverse temperatures  $T_{\parallel} \neq T_{\perp}$ . The vorticity source  $S_{\omega}(\chi, \theta, \varphi, v_{G\parallel}, \mu)$  introduced in Eq. (1) captures these basic properties (temperature anisotropy without density source), and effectively polarizes the plasma, as explained hereafter.  $T_s$  is the source temperature to which are normalized velocity space variables:  $\bar{\mu} = \mu/T_s$ ,  $\bar{v}_{G\parallel} = v_{G\parallel}/\sqrt{2T_s}$ .  $S_{\omega}$  then reads

$$S_{\omega} = [1 - \bar{\mu} B + (2\bar{v}_{G\parallel}^2 - 1)] S_r(\chi) S_{\omega 0} e^{-\bar{v}_{G\parallel}^2 - \bar{\mu} B}, \quad (4)$$

$S_r$  defines the radial profile of  $S_{\omega}$ , and  $S_{\omega 0}$  its normalized amplitude.

The time evolution of vorticity derives from the gyro-average of Eq. (1), integrated over velocity space and flux surface [25]:

$$\partial_t W + \partial_{\chi} \mathcal{K} = S_{\omega 0} \nabla_{\perp}^2 S_r. \quad (5)$$

$\mathcal{K}$  is the flux of vorticity,

$$\mathcal{K} = e \left\langle \int d\nu^* J \cdot \{ (d_t \mathbf{x}_G \cdot \nabla \chi) \bar{F} \} \right\rangle_{\text{fs}}. \quad (6)$$

Equation (5) shows that  $S_{\omega}$  acts as a source term for the electric field, as expected. To separate the effect of heating from that of polarization, we deliberately chose a source which does not inject total energy, by taking advantage of the possibility to independently control the amount of parallel energy. Relaxing this point would not modify qualitatively the results presented here. As in IBW experiments, the resulting vorticity source Eq. (4) leads to anisotropic temperature, that will reveal to be critical for the TB dynamics. Finally, the retained vorticity source does not inject any momentum in the system.

In this Letter, we focus on one simulation which is representative of the complex transport dynamics in the presence of a vorticity source. It is analogous to the series of simulations scanning the magnitude of both heat and vorticity sources, reported in [26]. The characteristic parameters are  $\rho_* \equiv \rho_0/a = 1/150$ , collisionality  $\nu_* = 0.1$ , and an aspect ratio of 3.2. The relatively low collisionality, which is in the ITER-relevant so-called banana regime, also ensures that collisions do not play a critical role in the results presented here.

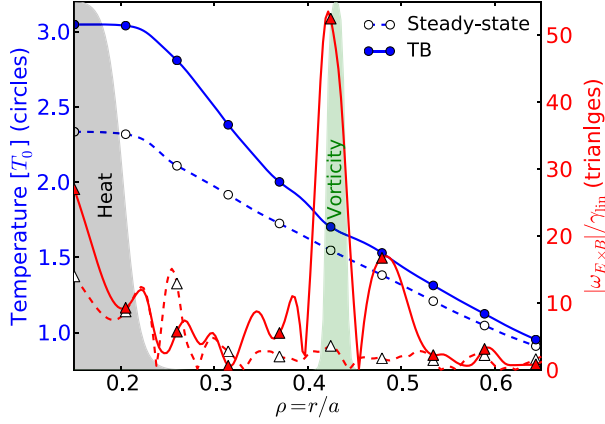


FIG. 1 (color online). Temperature (blue circles) and  $E \times B$  shear (red triangles) during steady-state (open) and a TB phase (solid). The kinetic sources are labeled by the black and green areas.

The heat source  $S_\varepsilon$  injects, in the inner part of the plasma, a power equivalent to  $P_{\text{add}} \sim 3.7$  MW for a deuterium plasma [8]. It leads to a temperature gradient slightly above the threshold for the ITG instability, in the range  $5 \lesssim R/L_T \lesssim 8$  over the whole radius before  $S_\omega$  is switched on. The radial domain of the simulation is defined by  $\rho \equiv r/a \in [0.15, 0.85]$ . The  $E \times B$  shear values are normalized to the maximal linear growth rate  $\gamma_{\text{lin}} = 0.075a/c_s$ —which we estimated during the initial stage of the simulation—in the following.

We first let the turbulence reach a statistical steady state ( $R/L_T \sim 7.3$  at the center), before the vorticity source is switched on at  $\tau_\omega \sim 2600a/c_s$  at the radial position  $\rho_\omega = 0.43$ . The temperature profile (blue circles) and the  $E \times B$  shear (red triangles) are displayed before (open symbols) and after (solid symbols) the introduction of the vorticity source in Fig. 1. The vorticity source (green area) position correlates well with the shear maximum, as expected. The induced  $E \times B$  shear is accompanied with the creation of a TB at  $\tau_1 = 5300a/c_s$ .

The effect of the vorticity source on turbulence is displayed in the top panel of Fig. 2. The detailed time evolution of the absolute value of the shearing rate  $\omega_{E \times B} \equiv (r/q)(d/dr)((q/r)(d\langle\phi\rangle_{\text{fs}}/dr))$  [27] at the source position  $\rho_\omega$  is given in the bottom panel. The sign of  $S_\omega$  is chosen so as to locally induce a shearing rate of the same sign as the intrinsic  $\omega_{E \times B}$ . As the turbulence gets increasingly quenched by the growing sheared electric field, the temperature gradient  $R/L_T$  (red dashed line) is able to grow: a TB is indeed slowly created as the absolute value of the shear increases.

Although we maintain the vorticity source constant in the simulation, we observe a quasiperiodic quenching of the shearing rate. The quenchantings happen at different values of  $\omega_{E \times B}$  and hence do not seem connected to a particular threshold in the poloidal shearing rate. In addition, the Reynolds stress at the origin of the shear

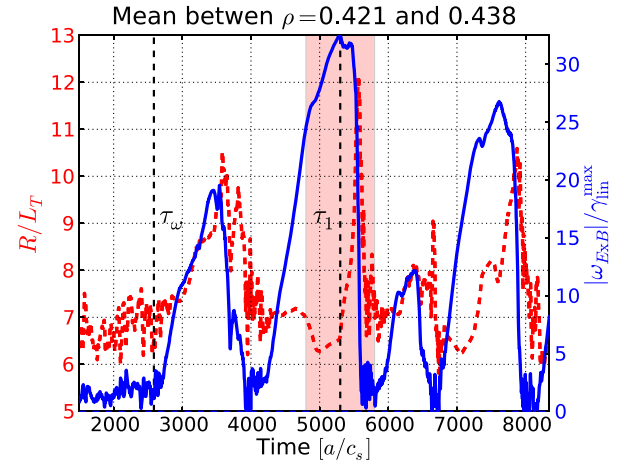
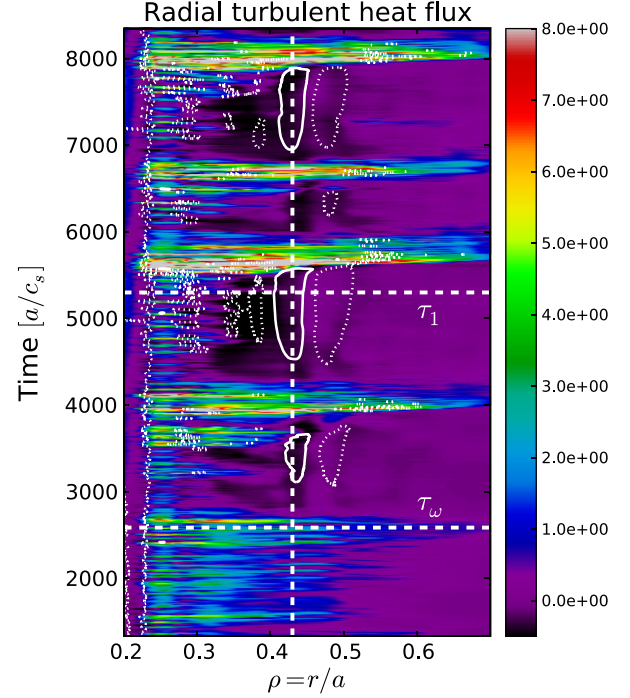


FIG. 2 (color online). Top. Turbulent heat flux (color map) and  $E \times B$  shearing rate contours (white contours: the dotted contour is  $8\gamma_{\text{lin}}$ , and the plain contour is  $-20\gamma_{\text{lin}}$ ). Bottom.  $E \times B$  shearing rate  $\omega_{E \times B}$  (plain blue line) and temperature gradient  $R/L_T$  (dashed red line) radially averaged close to  $\rho_\omega$ . The red area corresponds to the zoom window used in Fig. 3.

destruction peaks at a different location than the maximum  $E \times B$  shear and is therefore not likely to be associated with a Kelvin-Helmholtz type instability [28].

During the quenching, the temperature gradient undergoes transient dynamics whose details are variable. Still, generic features emerge. The temperature profile abruptly relaxes after this dynamics on approximately  $100a/c_s$  (roughly a few ms in ITER), and the temperature gradient recovers its typical initial values (we refer to this event as a crash in the remainder of this Letter). The first crash happens with a certain time delay compared to the

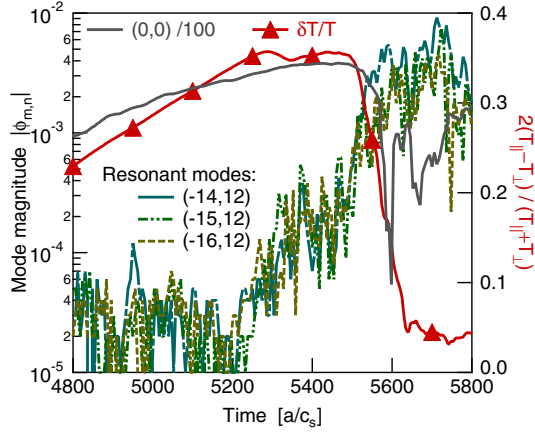


FIG. 3 (color online). Time evolution of the local resonant Fourier  $(m, n)$  modes left to the TB ( $\rho = 0.41$ ), during the second quenching. The temperature anisotropy is displayed in thin black line.

quenching of  $\omega_{E \times B}$ . Large-scale intense outward bursts of heat (top panel) then propagate throughout the whole radial domain as the barrier crashes.

We need to recall here that the vorticity source Eq. (4) heats the plasma in the parallel direction and cools it in the perpendicular direction. This induces a temperature anisotropy on a time scale comparable to the time scale of the sheared electric field creation. The temperature anisotropy always remains (below  $<35\%$ , cf. Fig. 3), and is clearly well within typical experimental ranges. It decreases the local linear threshold of the ITG modes at the position where both  $(T_{\parallel} - T_{\perp})/2T$  and  $\partial_r[(T_{\parallel} - T_{\perp})/2T]$  increase (vice versa, the threshold increases if the anisotropy and the gradient of the anisotropy both decrease [29]). Depending on the vorticity source sign, ITG modes are, consequently, excited on one side of the barrier and damped on the other side (both cases actually compare very well and lead to similar dynamics). In the case presented here, resonant modes can significantly grow on the inner side of the TB and participate to both the turbulent heat transport and to the turbulent flux of vorticity that appears in Eq. (5). This growth of ITG modes at  $\rho = 0.41$  is indeed observed in the simulation. The evolution of the resonant modes amplitude for the second quenching event in the simulation is displayed in Fig. 3. The local resonant modes start to grow exponentially before the electric field shear stops growing (red line), and saturate just after the crash. As expected, they stop growing when the temperature anisotropy is suppressed.

The growing ITG modes contribute to the turbulent Reynolds stress and efficiently screen the local  $E \times B$  shear induced by the vorticity source. In this case, the associated zonal flows are not inhibited by the large scale sheared flow. Additionally, the erosion of the shear is a positive feedback to the growth of ITG modes because it reduces the stabilization of the turbulent modes which can develop even more easily.

The growing modes also participate to the heat transport and tend to flatten the temperature gradient. The TB is then weakened, and the large amount of energy that was accumulated during the barrier creation phase in the inner part of the plasma is released in a massive heat burst (at  $t \sim 5600a/c_s$ ). The TB is destroyed and the electric field is drastically reduced throughout the whole plasma volume to its “pre-TB” state. Finally, the vorticity source that is still acting can drive again a sheared flow and the same process may repeat quasiperiodically.

Modeling the plasma on the system scale proves to be necessary to account for the action of the vorticity source. Indeed, flux-driven turbulence exhibits large-scale transport events referred to as avalanches [8,30]. As the heat source is increased, the avalanches become more frequent and more intense. Locally, at the source position, there is a competition between the effect of the vorticity source that tends to modify the radial electric field, and the net effect of the turbulent Reynolds Stress generated by the avalanches. In the simulation presented here, the vorticity source amplitude is sufficient to locally overcome the turbulent effects and is then able to induce a significantly different radial electric field. We performed a parameter scan in vorticity source amplitude and heat source amplitude, both scans confirming the existence of a threshold at which the vorticity source amplitude becomes large enough to compete with the turbulent Reynolds stress and to trigger the quasiperiodic creation and relaxation of TBs [26].

In this Letter, we have found a new mechanism that may explain TB relaxations in tokamak plasmas, an more precisely those generated by ICRH when ion Bernstein waves are excited. Externally generating sheared electric field via vorticity injection in flux-driven gyrokinetic simulations leads to the self-consistent triggering of a TB. We have demonstrated that the plasma polarization may imply the development of a temperature anisotropy which is responsible for the quasiperiodic relaxations of the TB. The basic mechanism can be understood as follows. (i) A sufficiently large vorticity source is applied to the plasma. (ii) Both the electric field and the temperature gradient grow, and (iii) a TB is created. In the meantime, (iv) should a secondary instability develop—either less sensitive to the ExB shearing than ITG turbulence, or on a different time scale—then relaxation dynamics can occur, as detailed hereafter. In the present case, it is the temperature anisotropy which leads to (v) the excitation of ITG modes on one side of the TB. (vi) These modes contribute to a Reynolds stress that screens the induced sheared electric field. The reason why they screen rather than add up remains to be clarified. The stabilizing effect of the associated sheared flow disappears and (vii) the TB is eroded by the turbulent heat transport. By switching off the source at various moments during this cycle, we found that this type of TB does not exhibit any hysteresis. Though, turning smartly on and off

the vorticity source could provide a way to inhibit the growth of the resonant modes and result in the creation of a steady-state TB. The essential feature for the existence of cyclic crashes is the fact that the source drives sheared flow, leading to the TB generation, and the secondary instability, governing the TB crash, evolves with separate dynamics due to different time scales and thresholds.

Releasing the adiabatic assumption for the electron response would offer turbulence an alternative channel to transport heat, as well as addressing the related particle transport issue in the presence of heat TB. Also, electromagnetic effects might play a role when TBs generate strong pressure gradients. All these important issues will be addressed in upgraded versions of the GYSELA code. The present work gives a clear physical picture that may be applied to shear-induced transport barriers observed in experiments with externally driven polarization (e.g., with ion Bernstein waves). Experimental attempts to better characterize this temperature anisotropy would thus be highly valuable as it may allow for the control of steady-state TBs in tokamaks.

The authors acknowledge fruitful discussions during “Festival de théorie” held in Aix-en-Provence, and enlightening discussion with R. Dumont on the properties of heating waves. This work was granted access to the HPC resources of TGCC and CINES under the allocation 2012052224 made by GENCI (Grand Equipement National de Calcul Intensif). This work was supported by EURATOM and carried out within the framework of the European Fusion Development Agreement. The views and opinions expressed herein do not necessarily reflect those of the European Commission.

---

\*Present address: Département de physique, Université de Montréal, C.P. 6128 Succ. Centre-Ville, Montréal, QC H3C-3J7, Canada.  
antoine.strugarek@cea.fr

- [1] H. Biglari, P.H. Diamond, and P.W. Terry, *Phys. Fluids B* **2**, 1 (1990).
- [2] X.-H. Wang, P.H. Diamond, and M.N. Rosenbluth, *Phys. Fluids* **4**, 2402 (1992).
- [3] S.B. Pope, *Turbulent Flows* (Cambridge University Press, Cambridge, England, 2000).
- [4] P.S. Marcus and S. Shetty, *Phil. Trans. R. Soc. A* **369**, 771 (2011).
- [5] M.E. McIntyre, *Chapter 1: The Atmospheric Wave-Turbulence Jigsaw, to appear in Rotation and Momentum Transport in Magnetised Plasmas*, edited by P. Diamond, X. Garbet, Ph. Ghendrih, and Y. Sarazin (World Scientific, Singapore, 2013).
- [6] D.E. Newman, B.A. Carreras, P.H. Diamond, and T.S. Hahm, *Phys. Plasmas* **3**, 1858 (1996).
- [7] E. Trier, L.-G. Eriksson, P. Hennequin, C. Fenzi, C. Bourdelle, G. Falchetto, X. Garbet, T. Aniel, F. Clairet, and R. Sabot, *Nucl. Fusion* **48**, 092001 (2008).
- [8] Y. Sarazin, V. Grandgirard, J. Abiteboul, S. Allfrey, X. Garbet, Ph. Ghendrih, G. Latu, A. Strugarek, and G. Dif-Pradalier, *Nucl. Fusion* **50**, 054004 (2010).
- [9] P.W. Terry, *Rev. Mod. Phys.* **72**, 109 (2000).
- [10] E.J. Doyle *et al.*, *Nucl. Fusion* **47**, S18 (2007).
- [11] X. Litaudon *et al.*, *Plasma Phys. Controlled Fusion* **38**, 1603 (1996).
- [12] B.P. Leblanc *et al.*, *Phys. Rev. Lett.* **82**, 331 (1999).
- [13] P.H. Diamond, S.-I. Itoh, K. Itoh, and T.S. Hahm, *Plasma Phys. Controlled Fusion* **47**, R35 (2005).
- [14] G. Dif-Pradalier, P.H. Diamond, V. Grandgirard, Y. Sarazin, J. Abiteboul, X. Garbet, Ph. Ghendrih, A. Strugarek, S. Ku, and C.S. Chang, *Phys. Rev. E* **82**, 025401(R) (2010).
- [15] E.-J. Kim and P.H. Diamond, *Phys. Rev. Lett.* **90**, 185006 (2003).
- [16] G. Dif-Pradalier, V. Grandgirard, Y. Sarazin, X. Garbet, and Ph. Ghendrih, *Phys. Rev. Lett.* **103**, 065002 (2009).
- [17] K. Miki, P.H. Diamond, Ö.D. Gürçan, G.R. Tynan, T. Estrada, L. Schmitz, and G.S. Xu, *Phys. Plasmas* **19**, 092306 (2012).
- [18] P. Manz *et al.*, *Phys. Plasmas* **19**, 072311 (2012).
- [19] X.Q. Xu *et al.*, *Nucl. Fusion* **42**, 21 (2002).
- [20] P. Beyer, S. Benkadda, G. Fuhr-Chaudier, X. Garbet, Ph. Ghendrih, and Y. Sarazin, *Phys. Rev. Lett.* **94**, 105001 (2005).
- [21] B.I. Cohen, T.J. Williams, A.M. Dimits, and J.A. Byers, *Phys. Fluids B* **5**, 2967 (1993).
- [22] B.F. McMillan, P. Hill, A. Bottino, S. Jolliet, T. Vernay, and L. Villard, *Phys. Plasmas* **18**, 112503 (2011).
- [23] V. Grandgirard *et al.*, *J. Comput. Phys.* **217**, 395 (2006).
- [24] G. Dif-Pradalier *et al.*, *Phys. Plasmas* **18**, 062309 (2011).
- [25] J. Abiteboul, X. Garbet, V. Grandgirard, S.J. Allfrey, Ph. Ghendrih, G. Latu, Y. Sarazin, and A. Strugarek, *Phys. Plasmas* **18**, 082503 (2011).
- [26] A. Strugarek *et al.*, *Plasma Phys. Controlled Fusion* **55**, 074013 (2013).
- [27] T.S. Hahm and K.H. Burrell, *Phys. Plasmas* **2**, 1648 (1995).
- [28] B.D. Scott, P.W. Terry, and P.H. Diamond, *Phys. Fluids* **31**, 1481 (1988).
- [29] J.-Y. Kim, W. Horton, D.I. Choi, S. Migliuolo, and B. Coppi, *Phys. Fluids B* **4**, 152 (1992).
- [30] Y. Idomura, H. Urano, N. Aiba, and S. Tokuda, *Nucl. Fusion* **49**, 065029 (2009).